Raw Materials for Geopolymer Production

Subjects: Materials Science, Characterization & Testing

Contributor: Jabulani Matsimbe, Megersa Dinka, David Olukanni, Innocent Musonda

Due to the high generation of industrial waste by-products, disposal concerns, less utilization, and hazardous nature, the research on its valorization as a precursor for geopolymer production is potentially environmentally viable.

Keywords: geopolymer ; geopolymer mortar ; geopolymer concrete ; inorganic polymers

1. Fly Ash

Fly ash is a major industrial fine particulate by-product formed from the combustion of coal and captured by electrostatic precipitators in thermal power plants. Coal fly ash annual production rates for major coal-consuming countries indicate approximately 600 million tonnes for China [1], 240 million tonnes for India [2], 32 million tonnes for the United States of America [3], 13 million tonnes for Australia [4], and 40 million tonnes for South Africa [5]. Fly ash is used in different applications or disposed of worldwide [6]. Due to its abundance, fly ash is one of the commonly used aluminosilicate sources used in geopolymer manufacturing [7][8][9]. **Table 1** gives the chemical composition of fly ash used in various parts of the world. The major compositions of the fly ash are SiO_2, Al_2O_3, Fe_2O_3, and CaO, while the minor constituents are MgO, P_2O_5, K_2O, Na_2O, SO_3, MnO, and TiO_2. The fly ash is classified as low calcium Class F, i.e., siliceous ash with pozzolanic properties as per ASTM C618, which specifies that the sum of SiO_2 + Al_2O_3 + Fe_2O_3 greater than 70 wt.% implies Class F and if the sum of SiO_2 + Al_2O_3 + Fe_2O_3 is between 50 wt.% and 70 wt.% implies Class C. In addition, ASTM C618 specifies that if the CaO content is less than 10 wt.%, the fly ash is classified as low calcium Class F, usually from bituminous coal. The SiO_2/Al_2O_3 ratio predicts the potential reactivity of ash as a supplementary cementitious material. The loss of ignition (LOI) of the fly ash samples is less than the LOI limit of 6% specified by ASTM C618 and this implies that the quantity of unburnt carbon in the ash and the performance of the boiler in the power plant are acceptable. **Figure 1** shows the morphology of fly ash which is a spherical smooth surface with relatively small particles [10] observed under a scanning electron microscope.

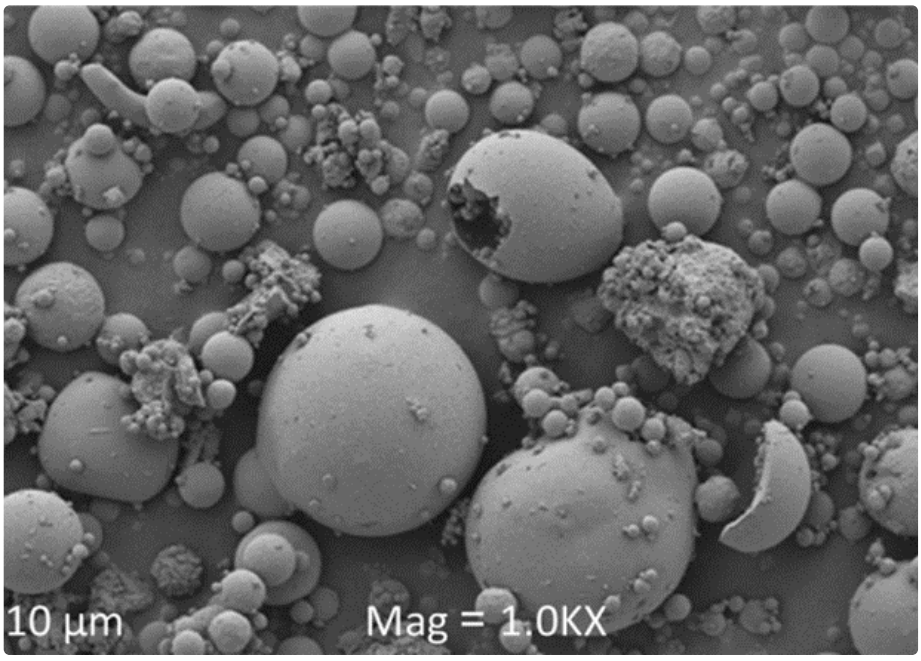

Figure 1. Morphology of fly ash [10].

Table 1. Chemical composition of fly ash in different areas of the world.

Country	Oxides (%)											
	SiO_2	Al_2O_3	Fe_2O_3	CaO	MgO	MnO	K_2O	Na_2O	TiO_2	P_2O_5	SO_3	LOI
South Africa [11]	56.45	30.27	3.58	4.59	1.06	-	0.77	0.14	1.57	0.38	-	0.42
India [8]	61.16	30.48	4.62	1.75	0.18	-	0.18	0.76	1.56	0.27	0.19	0.60
China [1]	54.6	27.2	11.6	2.2	1.0	-	0.7	1.0	0.5	-	-	1.0
Australia [12]	51.11	25.56	12.48	4.3	1.45	0.15	0.7	0.77	1.32	0.885	0.24	0.57
United Kingdom [13]	46.78	22.52	9.15	2.24	1.33	0.05	4.09	0.89	1.05	-	0.90	3.57
United States of America [14]	56.52	22.75	4.56	8.53	2.64	-	1.16	0.69	-	-	0.4	0.35

Naghizadeh et al. [11] studied the behavior of fly ash geopolymer binders exposed to various alkaline media. The study used low calcium Class F South African fly ash as the main precursor and mixed it with sodium silicate and 12 M sodium hydroxide to prepare the geopolymer binder. The mortar mixture contained a 2.25 aggregate/binder ratio, alkali activator solution of SiO_2/Na_2O = 1.4, and activator/FA ratio = 0.5. The 14 days' compressive strength at 80 °C curing temperature of the non-immersed, water immersed, 1 M NaOH mortar, and 3 M NaOH immersed mortar were 53.2 MPa, 50.6 MPa, 48.9 MPa, and 14.6 MPa, respectively. The decrease in the strength was attributed to the dissolution of Si and Al from the aluminosilicate gel network under an alkali attack. These results showed that severe alkali attack on fly ash-based geopolymer binder only occurs at alkali concentrations equal to/greater than 3 M NaOH. In another study, Rajmohan et al. [8] reported the mechanical and durability performance of heat-cured low calcium fly ash-based sustainable geopolymer concrete. In the study, the 28-day compressive strength before and after exposure to sulfate solution at 60 °C curing temperature was 56.18 MPa and 42.58 MPa; at 80 °C was 55.46 MPa and 44.92 MPa; at 100 °C was 50.79 MPa and 41.46 MPa, respectively. These results demonstrate that the fly ash-based geopolymer concrete gives adequate compressive strength and improved resistance to sulfate and acid attacks.

2. Phosphogypsum

Phosphogypsum (PG) is an industrial by-product of the wet-process production of phosphoric acid through the reaction of phosphate ore and sulphuric acid. PG annual production rates for major fertilizer manufacturing countries indicate approximately 50 million tonnes for China [15], 11 million tonnes for India [16], 40 million tonnes for the United States of America [17], and 35 million tonnes for South Africa [18]. Due to its abundance, other researchers have reused PG as a construction/building material [19][20][21], and soil stabilization material [18]. **Table 2** gives the chemical composition of phosphogypsum used in various parts of the world. The major compositions of the PG are CaO and SO_3. **Figure 2** shows the morphology of phosphogypsum which is of dense crystalline structure and irregularly shaped parallelepipeds [22] observed under a scanning electron microscope.

Figure 2. Morphology of phosphogypsum [22].

Table 2. Chemical composition of phosphogypsum in different areas of the world.

Country	Oxides (%)												%
	SiO_2	Al_2O_3	Fe_2O_3	CaO	MgO	MnO	K_2O	Na_2O	TiO_2	P_2O_5	SO_3	F	LOI
South Africa [18]	1.37	0.23	0.121	44	-	-	-	-	-	1.28	51	1.06	-
India [16]	1.75	0.13	0.16	38.87	0.02	-	-	0.11	0.05	1.04	52.94	0.32	3.97
China [15]	4.86	4.38	-	31.05	0.26	-	0.41	-	0.2	3.57	30.95	-	22.91
United Kingdom [17]	2.4	0.40	0.23	40	0.04	-	0.03	0.13	0.03	0.95	52	0.14	6.40
United States of America [17]	3	0.3	0.2	31	-	-	-	-	0.04	2.25	55	0.2	17.7

Hua et al. [15] studied the effects of fibers on mechanical properties and freeze–thaw resistance of phosphogypsum-slag-based geopolymer and found that the addition of 1% fiber increased the flexural strength from 7.9 MPa and 8.4 MPa (0% fiber) to 9.5 MPa and 12.5 MPa at 7 and 28 days, respectively. The alkaline activator was prepared using sodium silicate (water glass) of modulus 3.0 and sodium hydroxide. The pastes were made with a water/powder ratio of 0.6. The results indicated in the study showed that polypropylene fiber provides a phosphogypsum-slag mix with better performance than mineral and glass fibers. In another study, Ref. [23] reported the x-ray diffraction and scanning electron microscopy of fly ash-phosphogypsum geopolymer bricks using 10 M sodium hydroxide and sodium silicate. For the 70–75 °C oven-cured samples for 12 h, the compressive strength was 20.31 MPa (9% PG content), 23.13 MPa (13% PG content), 23.06 MPa (14% PG content), and 15.13 MPa (25% PG content) showing that an increase in PG content beyond 13% lead to a decrease in compressive strength. For the 24 h air-cured samples, the compressive strength was 18.31 MPa (9% PG content), 21.38 MPa (13% PG content), 21.37 MPa (14% PG content), and 13.92 MPa (25% PG content) showing that an increase in PG content beyond 13% lead to a decrease in compressive strength. The results showed that the FA-PG geopolymer bricks with higher compressive strength can be used for building applications, whilst those with lower compressive strength can be used as filler material. Rashad [24] studied the potential use of calcined phosphogypsum (CPG) (heated at 850 °C for 2 h) in alkali-activated fly ash (FA) under the effects of elevated temperatures and thermal shock cycles. The 28 days compressive strength of the FA/CPG mix proportions of 100/0, 95/5, 90/10, and 85/15 using sodium silicate as alkali activator (density 1.38 g/cm^3, 8.2% Na_2O, 27% SiO_2, 64% H_2O) cured at 75 °C for 7 days then ambient cured for the extra 21 days was 14.95 MPa, 26 MPa, 23 MPa, and 12.5 MPa, respectively. The increase in compressive strength at 5 and 10% CPG inclusion is attributed to a reduction in apparent porosity and un-hydrated particles, giving a relatively dense and interlocking structure. The rapid decrease in compressive strength at 15% CPG inclusion is attributed to a flocculent and porous structure that gives euhedral prismatic crystals of gypsum, which act as a barrier against geopolymer chain formation and thus reducing the cohesion of the microstructure. The residual strength increased with increasing heat treatments. The results indicate the possibility of recycling phosphogypsum in an alkali-activated fly ash system such as an ordinary Portland cement system. In another study, Ref. [25] reported the production of geopolymer binders at room temperature using calcined clay, waste brick, PG (4%, 8%, 12%, and 16%), and sodium hydroxide alkali activator (10 M, 14 M, and 17 M) with a solid/liquid ratio of 3. The highest 28-day compressive strength of 36 MPa was achieved at 8% PG replacement and 14 M sodium hydroxide, after which the calcined clay was replaced by waste brick (WB) powder which achieved similar mechanical properties as the optimal condition. An increase in phosphogypsum content above 8% decreased the compressive strength due to the excess sulfate disturbing the geopolymer structure by forming ettringite which causes swelling through moisture absorption. The results foster the utilization of low-cost waste materials (PG and WB) for geopolymer binder production and further recommend studying the fire resistance, acid attack, chloride attack, sulfate attack, and permeability.

3. Bottom Ash

As compared to fly ash, bottom ash is collected at the bottom of the boiler and has coarser, angular, large-sized particles with a greater content of unburned carbon [26]. **Figure 3** shows the SEM image of bottom ash which has coarser, irregular large-sized angular particles.

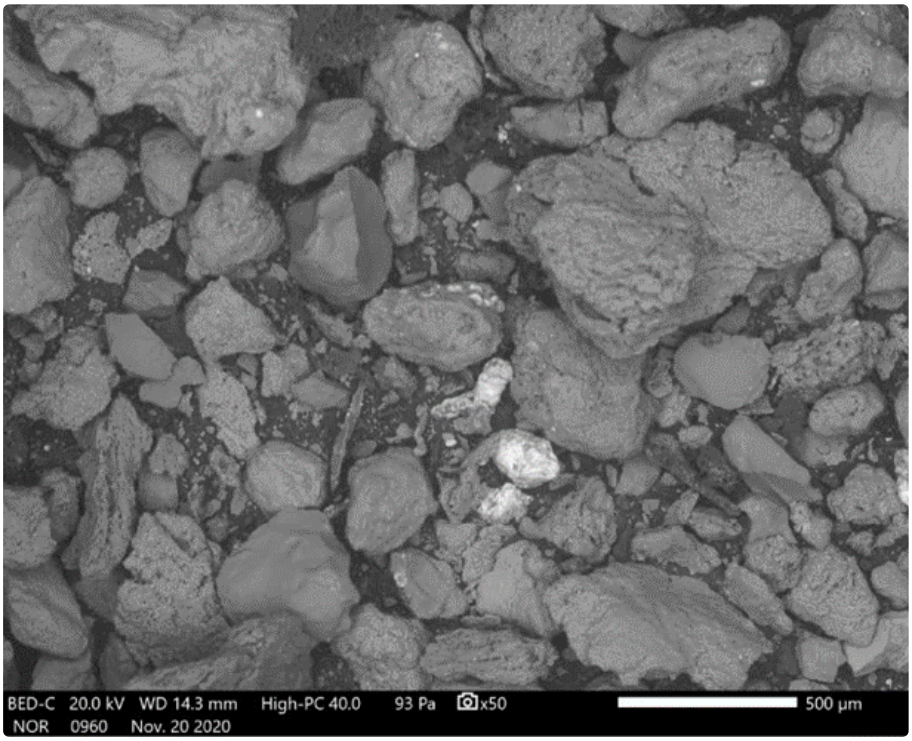

Figure 3. SEM image of bottom ash [26].

Despite its inferior properties, several geopolymer research incorporating bottom ash has been conducted. Ref. [27] studied the behavior of low-calcium fly and bottom ash-based geopolymer concrete cured at ambient temperature. In the study, the compressive strength of coal ash-based geopolymer concrete increased with a decrease in the liquid-to-binder ratio or an increase in the mass ratio of the fly ash-to-bottom ash. In another study, Ref. [28] reported the properties of cellular lightweight high calcium bottom ash-Portland cement geopolymer mortar. The results showed that the compressive strength increased with an increase in the binder and sodium hydroxide content but decreased with an increase in the foam content.

4. Ground Granulated Blast Furnace Slag

Ground granulated blast furnace slag (GGBFS) is a granular by-product material from the production of iron. **Figure 4** shows that the XRD of GGBFS consists of an amorphous phase shown by a hump around 25–35°2 theta with a small amount of Fe_3O_4, whilst the XRD of FA consist of an amorphous phase shown by a hump around 18–28°2 theta with some crystalline phases of $Al_6Si_2O_{13}$, SiO_2, magnesioferrite, and CaO [29]. Due to its glassy phase nature and calcium content, GGBFS is easier to activate through alkali activation and forms C-S-H or C-A-S-H gels as chemical reaction products which improve the geopolymer strength just as in ordinary Portland cement (OPC).

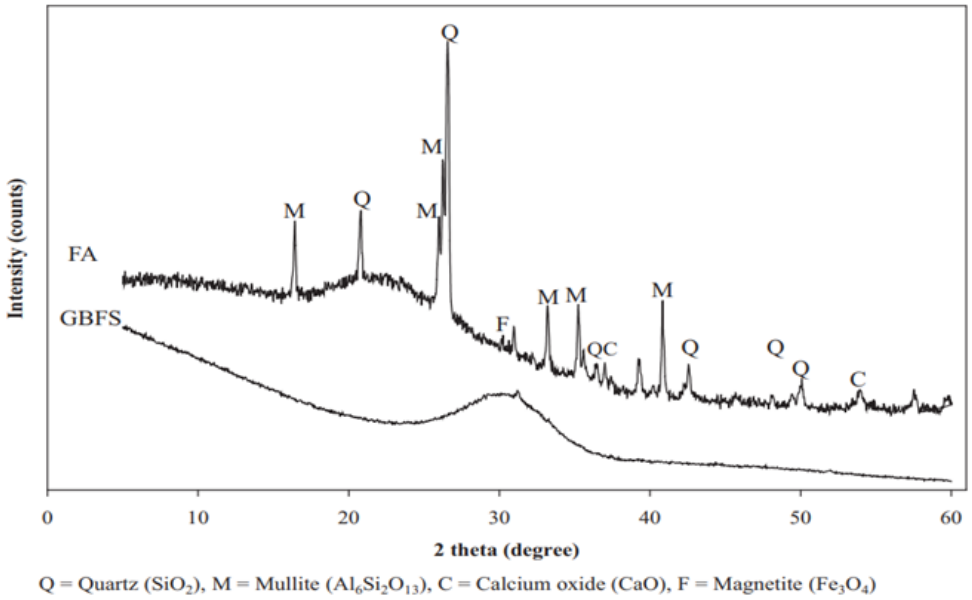

Figure 4. Comparative XRD of GGBFS and FA [29].

Calcium alumino-silicate hydrate (C-A-S-H) gel is the main reaction product during GGBFS activation, giving enhanced early strength development and reduced setting time in ambient curing conditions [30][31]. Aziz et al. [32] studied the strength development of solely GGBFS geopolymers and found that the 28 days compressive strength of 168.7 MPa was achieved with a solid/liquid ratio of 3.0, alkaline activator ratio of 2.5, and formation of tobermorite and calcite. Sithole et al. [33] studied the feasibility of synthesizing geopolymer bricks through alkaline activation of GGBFS and found that the 5 days compressive strength at 80 °C curing temperature, 15 M sodium hydroxide, and 0.15 liquid/solid ratio was 72 MPa attributed to the formation of a dense, less porous, and more amorphous microstructure. The geopolymer brick met the minimum compressive strength of 20.7 MPa, and water absorption of less than 17% as per ASTM C126-99 and ASTM C216-07a, respectively, for usage as facing and solid masonry brick. In another study, Ref. [34] reported the effect of GGBFS inclusion on the reactivity and microstructure properties of fly ash-based geopolymer concrete cured in ambient conditions. The 28-day compressive strengths of 30 MPa, 35 MPa, 40 MPa, and 45 MPa were achieved at 0%, 10%, 20%, and 30% replacement levels, respectively, attributed to the formation of calcium silicate hydrate (C-S-H) gel when increasing the GGBFS percentage levels.

5. Basic Oxygen Furnace Slag

Basic oxygen furnace slag (BOFS) is a by-product material from the production of steel. **Figure 5** shows that the morphology of BOFS is composed of non-spherical glassy irregularly shaped microstructures. The observed rougher and cloudy texture surface is attributed to the presence of CaO [35].

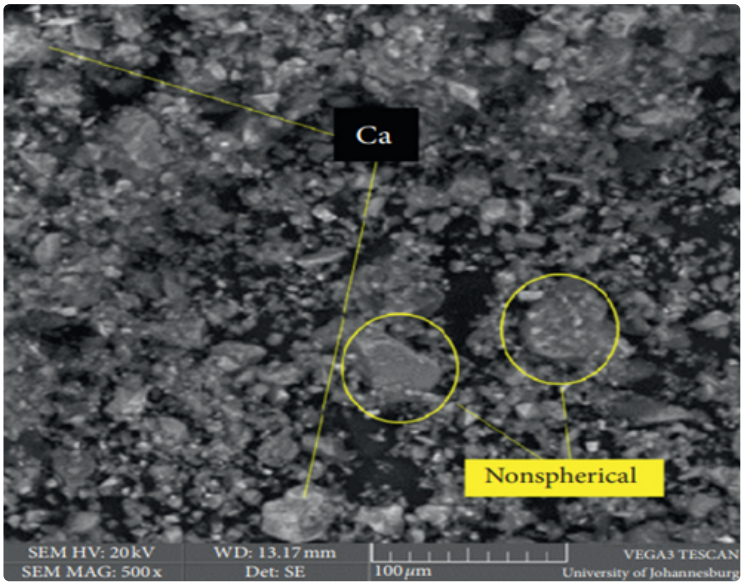

Figure 5. SEM image of BOFS [35].

Sithole et al. [36] studied the mechanical performance of fly ash modified BOFS-based geopolymer masonry bricks and concluded that to meet the ASTM C34-13 for masonry bricks, the most favorable conditions for the geopolymer synthesis were 10% fly ash, 5M sodium hydroxide, and 80 °C curing temperature. In another study, Mashifana et al. [35] explored the utilization of BOFS and gold mine tailings (GMT) for geopolymer synthesis and found that the 5 days compressive strength of the GMT: BOFS geopolymer cured at 90 °C was 20 MPa and 25.7 MPa for sodium hydroxide and potassium hydroxide alkaline activators, respectively, which satisfied the ASTM 34-17a and SANS 227:2007 for burnt masonry units, mine backfill paste, and lightweight civil works. Lee et al. [37] reported the stabilization of BOFS geopolymer and found that the 28-day compressive strength was 30–40 MPa, and its expansion was less than 0.5% after the ASTM C151 autoclave testing. The results show that slag can be turned into a value-added product through green geopolymer composites.

6. Silica Fume

Silica fume is an ultrafine by-product powder from the production of elemental silicon and ferrosilicon alloy in electric arc furnaces. Li et al. [38] studied the rheological and viscoelastic characterizations of fly ash/slag/silica fume-based geopolymer and concluded that the use of 20–30% silica fume to partially replace slag reduces the shear stress of fly ash-slag-based geopolymer grouting material. The results indicated that geopolymer instead of ordinary Portland cement paste can be used as a grouting material, and further recommend studying the shrinkage and creep of geopolymer grouting material. In another study, Duan et al. [39] observed that the inclusion of silica fume from 10–30% replacement levels increased the compressive strength of geopolymer, attributing it to the increase in chemical reaction products leading to a more dense, compact, and homogeneous microstructure. Similar results were observed by [40]. **Figure**

6 shows the correlation between the Si/Al ratio and the compressive strength, which is directly proportional. The dissolution of the silica fume in the blended mixture leads to a further increase in the Si/Al ratio in the aluminosilicate gel and thus increases the compressive strength.

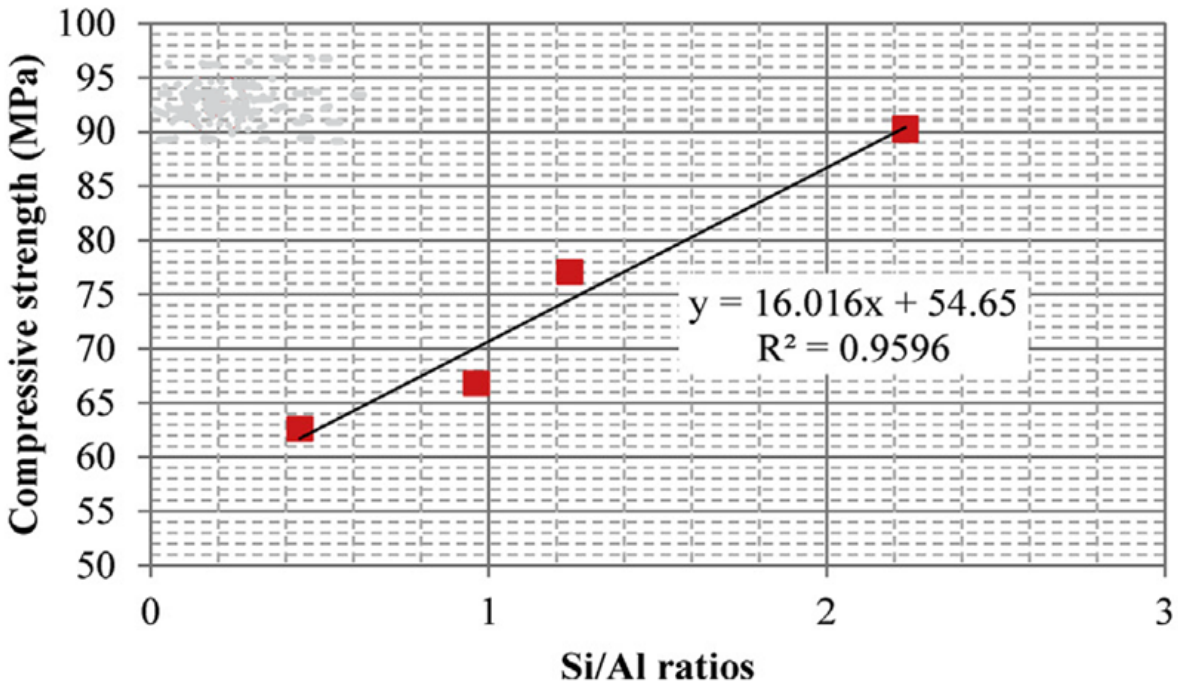

Figure 6. Compressive strength in the function of the Si/Al ratios [39].

7. Flue gas desulphurization gypsum

Flue gas desulphurization gypsum (FGDG) is an industrial by-product produced through limestone-gypsum wet desulphurization of coal-fired flue gas with calcium sulfate dihydrate ($CaSO_4 \cdot 2H_2O$) as the main product [41]. Guo et al. [42] studied the utilization of thermally treated FGDG and fly ash (FA) in geopolymer preparation and found that geopolymer containing 90% FA and 10% FGDG thermally treated at 800 °C for 1 h gave a better compressive strength of 37 MPa.

8. Red Mud

Red mud (bauxite residue) is a by-product generated during bauxite ore processing into alumina through the Bayer process. Sun et al. [43] studied the mechanical and environmental characteristics of red mud geopolymers and found that the 28-day compressive strength of red mud geopolymers ranged from 35.2 MPa to 68.7 MPa. The leaching of heavy metal and trace elements met the thresholds of cementitious materials. In the study, it was recommended that future work should study the chemical states, the influence of pore structure, and the pore solution of red mud geopolymers. The mechanical properties of red mud geopolymers are affected by source material properties, alkaline activator concentration, and curing conditions [44][45].

9. Mine Tailings

Falayi [46] reported the comparison between fly ash (FA) and basic oxygen furnace slag (BOFS) modified gold mine tailings (GMT) geopolymer and found that BOFS-GMT geopolymer and FA-GMT geopolymer gave compressive strengths of 21.44 MPa and 12.98 MPa cured at 70 °C and 90 °C, respectively. The higher strength in BOFS geopolymer was attributed to the formation of C-A-S-H gel.

10. Rice Husk Ash

Rice husk ash is a by-product of burning rice husk as a fuel source in boilers to generate electricity. Somna et al. [10] utilized rice husk ash (RHA) to produce RHA-FA geopolymer hollow block and concluded that the increase in RHA content increased the geopolymer compressive strength. In the study, the mix proportion of 50%FA:50%RHA with 14 M sodium hydroxide gave the preferred 28-day compressive strength of 8.5 MPa, which satisfied the TIS 58-2560 standard for usage in concrete hollow block manufacturing. Another study by [47] concluded that the use of RHA in geopolymer production is a sustainable and eco-friendly route for the construction industry. However, the sustainability and the eco-

friendly route are questionable considering the caustic nature and high cost of the hydroxides and silicates used for the activation process. The sustainability part comes in from the reuse of the waste which would have otherwise been landfilled and leached into groundwater. Basri et al. [48] observed that an RHA/AA range of 0.7–0.8 and NaOH between 12–14 M increased the geopolymer compressive strength upwards of 23 MPa. They further found that the Fourier transform infrared spectroscopy (FTIR) spectra of RHA, shown in **Figure 7**, had a relatively high ratio of the inverted peak height (H) and the inverted peak (AS) of Si-O-Si stretching vibration. This implies that both S23 (brittle) and S28 (ductile) samples underwent high geopolymerization, which produced a higher compressive strength.

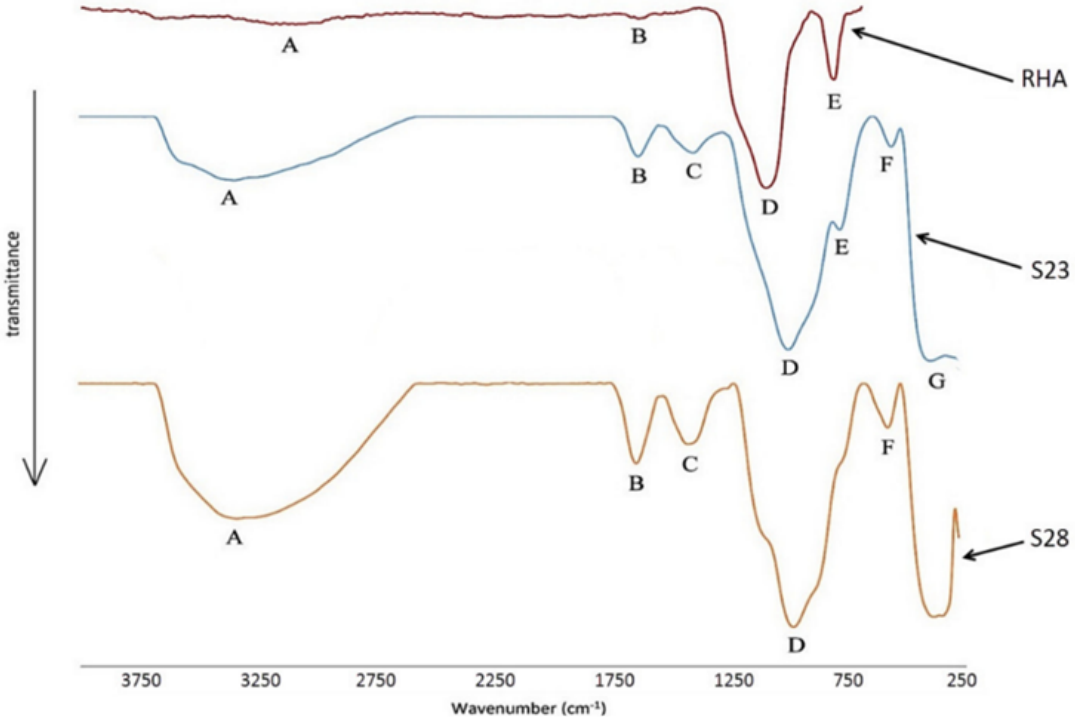

Figure 7. FTIR spectra of RHA [48].

11. Palm Oil Fuel Ash

Palm oil fuel ash (POFA) is an industrial waste collected from the combustion of palm oil waste as fuel to generate electricity. Ranjbar et al. [49] studied the compressive strength and microstructural analysis of FA-POFA-based geopolymer mortar and found that the increase in POFA/FA ratio increased the SiO_2/Al_2O_3 ratio leading to a decrease in early age strength and later gradual strength gains attributed to the reaction of aluminate species in early stages/scarcity of Al at later stages, and dominance in the reaction of silicate species at later stages. Similar results were obtained by [50], who attributed the loss in strength to a decrease in the dense gel formation and changes in crystallinity as the POFA replacement levels increased from 50–70% by weight of GGBFS. **Figure 8** shows the FTIR of alkali-activated materials prepared with different levels of POFA. After adding POFA at 50, 60, and 70% replacement levels, the stretching vibrations of Si-O-Al emerged at 956.9, 963.1, and 964.8 cm^{-1}, respectively. The mixtures showed significant structural alterations due to higher content of SiO_2 and a decrease in C-(N)-A-S-H and C-S-H gel production leading to a decrease in mechanical strength and delayed geopolymerization process.

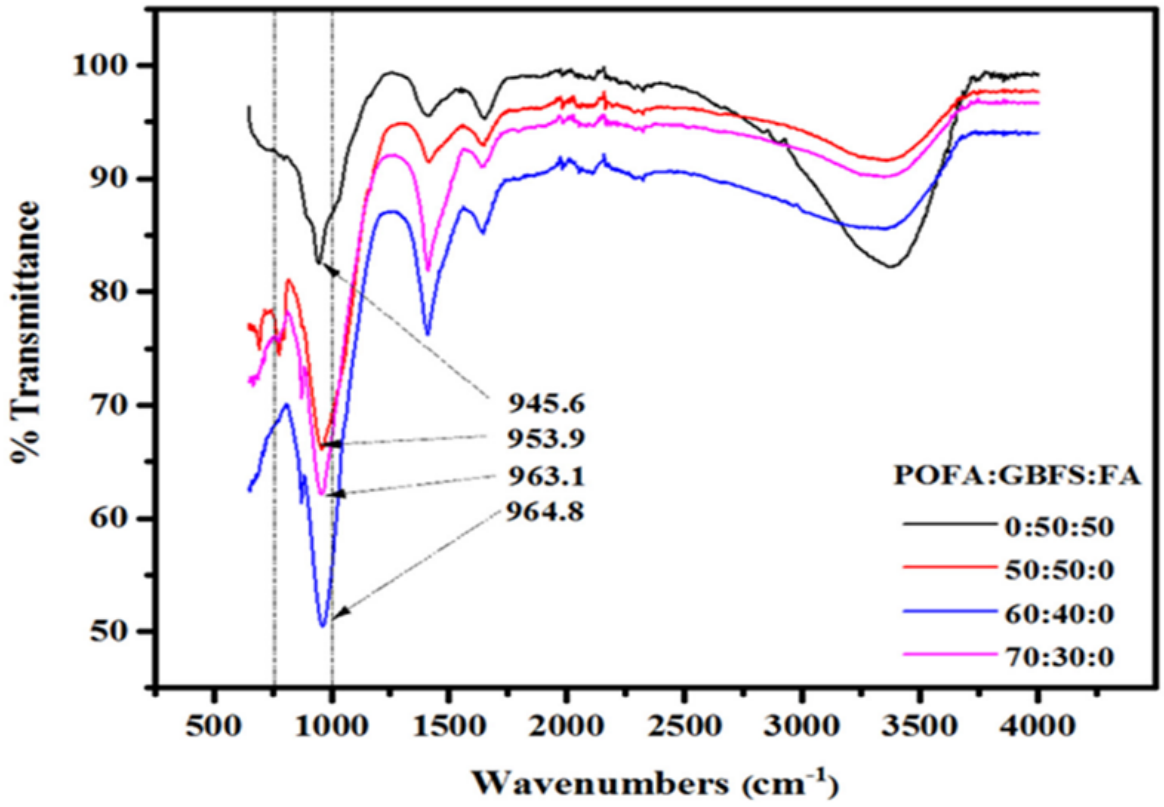

Figure 8. FTIR of AAMs with different POFA levels [50].

12. Waste Glass

The manufacturing and consumption of glass have increased globally due to an advancement in the standards of living. Waste glass (WG) is non-biodegradable and non-combustible, thus leading to increased landfills. Due to its high amorphous silica content, waste glass powder has the potential to be used as a silica source just as fly ash. Xiao et al. [51] studied the strength of waste glass geopolymers cured at ambient temperature and found that the geopolymer obtained by mixing 25WG:75FA (WG/FA = 1:3) at a Si/Al ratio of 3.038 and 5 M sodium hydroxide gave a compressive strength of 34.5 Mpa making it suitable for usage as a precursor in geopolymer production. In another study by [52], waste glass powder replaced 10 to 40% of Class C fly ash to produce geopolymer paste cured at 60 °C for 48 h and then held at room temperature (23 °C) giving a 7-day compressive strength range of 34–48 Mpa. The 10–20% replacement levels by weight yielded the best optimum mechanical results. Similar results were obtained by [53], who attributed the improved compressive strength performance to reactive SiO_2 and Al_2O_3, contributing to the generation of N-A-S-H gel. **Figure 9** shows the SEM images of ground fluorescent lamp glass (FP) and ground container glass (CP) powders [52] having irregular angular particles, smooth surfaces, and sharp edges.

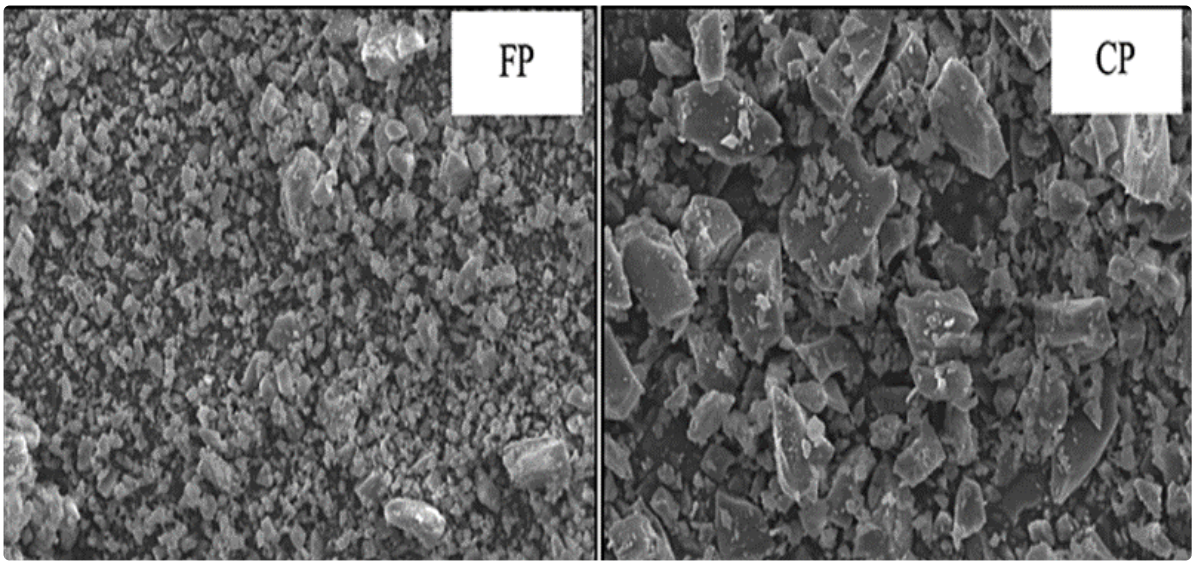

Figure 9. SEM image of waste glass power [52].

References

1. Chen, K.; Wu, D.; Zhang, Z.; Pan, C.; Shen, X.; Xia, L.; Zang, J. Modeling and optimization of fly ash–slag-based geopolymer using response surface method and its application in soft soil stabilization. Constr. Build. Mater. 2021, 315, 125723.
2. Harris, D. Ash as an internationally traded commodity. In Coal Combustion Products (CCP's); Robl, T., Oberlink, A., Jones, R., Eds.; Elsevier: Amsterdam, The Netherlands, 2017; pp. 509–529.
3. Ash at Work: Applications, Science, and Sustainability of Coal Ash; ACAA: Farmington Hills, MI, USA, 2021.
4. Amran, M.; Debbarma, S.; Ozbakkaloglu, T. Fly ash-based eco-friendly geopolymer concrete: A critical review of the long-term durability properties. Constr. Build. Mater. 2020, 270, 121857.
5. Mashifana, T.; Sithole, N. Utilization of fly ash: Basic oxygen furnace slag as a raw material in geopolymerization. IOP Conf. Series: Mater. Sci. Eng. 2019, 652, 012060.
6. Ismail, I.; Bernal, S.A.; Provis, J.L.; San Nicolas, R.; Hamdan, S.; van Deventer, J.S.J. Modification of phase evolution in alkali-activated blast furnace slag by the incorporation of fly ash. Cem. Concr. Compos. 2014, 45, 125–135.
7. Naghizadeh, A.; Ekolu, S. Method for comprehensive mix design of fly ash geopolymer mortars. Constr. Build. Mater. 2019, 202, 704–717.
8. Rajmohan, B.; Nayaka, R.R.; Kumar, K.R.; Kaleemuddin, K. Mechanical and durability performance evaluation of heat cured low calcium fly ash based sustainable geopolymer concrete. Mater. Today: Proc. 2022, 58, 1337–1343.
9. Zhuang, X.Y.; Chen, L.; Komarneni, S.; Zhou, C.H.; Tong, D.S.; Yang, H.M.; Yu, W.H.; Wang, H. Fly ash-based geopolymer: Clean production, properties and applications. J. Clean. Prod. 2016, 125, 253–267.
10. Somna, R.; Saowapun, T.; Somna, K.; Chindaprasirt, P. Rice husk ash and fly ash geopolymer hollow block based on NaOH activated. Case Stud. Constr. Mater. 2022, 16, e01092.
11. Naghizadeh, A.; Ekolu, S.O. Behaviour of fly ash geopolymer binders under exposure to alkaline media. Asian J. Civ. Eng. 2019, 20, 785–798.
12. Graytee, A.; Sanjayan, J.G.; Nazari, A. Development of a high strength fly ash-based geopolymer in short time by using microwave curing. Ceram. Int. 2018, 44, 8216–8222.
13. Aiken, T.A.; Kwasny, J.; Sha, W. Resistance of fly ash geopolymer binders to organic acids. Mater. Struct. 2020, 53, 115.
14. Alanazi, H.; Hu, J.; Kim, Y.-R. Effect of slag, silica fume, and metakaolin on properties and performance of alkali-activated fly ash cured at ambient temperature. Constr. Build. Mater. 2018, 197, 747–756.
15. Hua, S.; Wang, K.; Yao, X.; Xu, W.; He, Y. Effects of fibers on mechanical properties and freeze-thaw resistance of phosphogypsum-slag based cementitious materials. Constr. Build. Mater. 2016, 121, 290–299.
16. Raut, S.P.; Patil, U.S.; Madurwar, M.V. Utilization of phosphogypsum and rice husk to develop sustainable bricks. Mater. Today: Proc. 2022, 60, 595–601.
17. Available online: http://www-pub.iaea.org/MTCD/Publications/PDF/Pub1582_web.pdf (accessed on 11 July 2022).
18. Mashifana, T.P.; Okonta, F.N.; Ntuli, F. Geotechnical Properties and Microstructure of Lime-Fly Ash-Phosphogypsum-Stabilized Soil. Adv. Civ. Eng. 2018, 2018, 3640868.
19. Cao, Y.; Cui, Y.; Yu, X.; Li, T.; Chang, I.-S.; Wu, J. Bibliometric analysis of phosphogypsum research from 1990 to 2020 based on literatures and patents. Environ. Sci. Pollut. Res. 2021, 28, 66845–66857.
20. Rashad, A.M. Phosphogypsum as a construction material. J. Clean. Prod. 2017, 166, 732–743.
21. Wei, Z.; Deng, Z. Research hotspots and trends of comprehensive utilization of phosphogypsum: Bibliometric analysis. J. Environ. Radioact. 2021, 242, 106778.
22. Vaičiukynienė, D.; Nizevičienė, D.; Kantautas, A.; Bocullo, V.; Kielė, A. Alkali Activated Paste and Concrete Based on of Biomass Bottom Ash with Phosphogypsum. Appl. Sci. 2020, 10, 5190.
23. Vijay, J.J.; Rao, H.S.; Ghorpade, V.G. XRD & SEM studies of Fly-ash and Phosphogypsum based Geopolymer Bricks. Int. J. Eng. Trends Technol. 2021, 69, 225–232.
24. Rashad, A.M. Potential use of phosphogypsum in alkali-activated fly ash under the effects of elevated temperatures and thermal shock cycles. J. Clean. Prod. 2015, 87, 717–725.
25. Hamdi, N.; Ben Messaoud, I.; Srasra, E. Production of geopolymer binders using clay minerals and industrial wastes. Comptes Rendus. Chim. 2018, 22, 220–226.

26. Fidanchevski, E.; Angjusheva, B.; Jovanov, V.; Murtanovski, P.; Vladiceska, L.; Aluloska, N.S.; Nikolic, J.K.; Ipavec, A.; Šter, K.; Mrak, M.; et al. Technical and radiological characterisation of fly ash and bottom ash from thermal power plant. J. Radioanal. Nucl. Chem. Artic. 2021, 330, 685–694.
27. Xie, T.; Ozbakkaloglu, T. Behavior of low-calcium fly and bottom ash-based geopolymer concrete cured at ambient temperature. Ceram. Int. 2015, 41, 5945–5958.
28. Suksiripattanapong, C.; Krosoongnern, K.; Thumrongvut, J.; Sukontasukkul, P.; Horpibulsuk, S.; Chindaprasirt, P. Properties of cellular lightweight high calcium bottom ash-portland cement geopolymer mortar. Case Stud. Constr. Mater. 2020, 12, e00337.
29. Phoo-Ngernkham, T.; Maegawa, A.; Mishima, N.; Hatanaka, S.; Chindaprasirt, P. Effects of sodium hydroxide and sodium silicate solutions on compressive and shear bond strengths of FA–GBFS geopolymer. Constr. Build. Mater. 2015, 91, 1–8.
30. Nath, P.; Sarker, P.K. Effect of GGBFS on setting, workability and early strength properties of fly ash geopolymer concrete cured in ambient condition. Constr. Build. Mater. 2014, 66, 163–171.
31. Nath, P.; Sarker, P. Fracture properties of GGBFS-blended fly ash geopolymer concrete cured in ambient temperature. Mater. Struct. 2016, 50, 32.
32. Aziz, I.H.; Abdullah, M.M.A.B.; Salleh, M.M.; Azimi, E.A.; Chaiprapa, J.; Sandu, A.V. Strength development of solely ground granulated blast furnace slag geopolymers. Constr. Build. Mater. 2020, 250, 118720.
33. Sithole, N.T.; Mashifana, T. Geosynthesis of building and construction materials through alkaline activation of granulated blast furnace slag. Constr. Build. Mater. 2020, 264, 120712.
34. Nagajothi, S.; Elavenil, S. Effect of GGBS Addition on Reactivity and Microstructure Properties of Ambient Cured Fly Ash Based Geopolymer Concrete. Silicon 2020, 13, 507–516.
35. Mashifana, T.; Sebothoma, J.; Sithole, T. Alkaline Activation of Basic Oxygen Furnace Slag Modified Gold Mine Tailings for Building Material. Adv. Civ. Eng. 2021, 2021, 9984494.
36. Sithole, N.; Okonta, F.; Ntuli, F. Mechanical Properties and Structure of Fly Ash Modified Basic Oxygen Furnace Slag Based Geopolymer Masonry Blocks. J. Solid Waste Technol. Manag. 2020, 46, 372–383.
37. Lee, W.-H.; Cheng, T.-W.; Lin, K.-Y.; Lin, K.-L.; Wu, C.-C.; Tsai, C.-T. Geopolymer Technologies for Stabilization of Basic Oxygen Furnace Slags and Sustainable Application as Construction Materials. Sustainability 2020, 12, 5002.
38. Li, L.; Wei, Y.-J.; Li, Z.; Farooqi, M.U. Rheological and viscoelastic characterizations of fly ash/slag/silica fume-based geopolymer. J. Clean. Prod. 2022, 354, 131629.
39. Duan, P.; Yan, C.; Zhou, W. Compressive strength and microstructure of fly ash based geopolymer blended with silica fume under thermal cycle. Cem. Concr. Compos. 2017, 78, 108–119.
40. Sukontasukkul, P.; Chindaprasirt, P.; Pongsopha, P.; Phoo-Ngernkham, T.; Tangchirapat, W.; Banthia, N. Effect of fly ash/silica fume ratio and curing condition on mechanical properties of fiber-reinforced geopolymer. J. Sustain. Cem. Mater. 2020, 9, 218–232.
41. Liu, S.; Liu, W.; Jiao, F.; Qin, W.; Yang, C. Production and resource utilization of flue gas desulfurized gypsum in China —A review. Environ. Pollut. 2021, 288, 117799.
42. Guo, X.; Shi, H.; Dick, W.A. Utilization of thermally treated flue gas desulfurization (FGD) gypsum and class-C Fly Ash (CFA) to prepare CFA-based geopolymer. J. Wuhan Univ. Technol. Sci. Ed. 2013, 28, 132–138.
43. Sun, Z.; Tang, Q.; Xakalashe, B.S.; Fan, X.; Gan, M.; Chen, X.; Ji, Z.; Huang, X.; Friedrich, B. Mechanical and environmental characteristics of red mud geopolymers. Constr. Build. Mater. 2022, 321, 125564.
44. He, J.; Zhang, J.; Yu, Y.; Zhang, G. The strength and microstructure of two geopolymers derived from metakaolin and red mud-fly ash admixture: A comparative study. Constr. Build. Mater. 2012, 30, 80–91.
45. Singh, S.; Aswath, M.; Ranganath, R. Effect of mechanical activation of red mud on the strength of geopolymer binder. Constr. Build. Mater. 2018, 177, 91–101.
46. Falayi, T. A comparison between fly ash- and basic oxygen furnace slag-modified gold mine tailings geopolymers. Int. J. Energy Environ. Eng. 2019, 11, 207–217.
47. Hossain, S.S.; Roy, P.; Bae, C.-J. Utilization of waste rice husk ash for sustainable geopolymer: A review. Constr. Build. Mater. 2021, 310, 125218.
48. Basri, M.S.M.; Mustapha, F.; Mazlan, N.; Ishak, M.R. Rice Husk Ash-Based Geopolymer Binder: Compressive Strength, Optimize Composition, FTIR Spectroscopy, Microstructural, and Potential as Fire-Retardant Material. Polymers 2021, 13, 4373.

49. Ranjbar, N.; Mehrali, M.; Behnia, A.; Alengaram, U.J.; Jumaat, M.Z. Compressive strength and microstructural analysis of fly ash/palm oil fuel ash based geopolymer mortar. Mater. Des. 2014, 59, 532–539.
50. Huseien, G.F.; Asaad, M.A.; Abadel, A.A.; Ghoshal, S.K.; Hamzah, H.K.; Benjeddou, O.; Mirza, J. Drying Shrinkage, Sulphuric Acid and Sulphate Resistance of High-Volume Palm Oil Fuel Ash-Included Alkali-Activated Mortars. Sustainability 2022, 14, 498.
51. Xiao, R.; Ma, Y.; Jiang, X.; Zhang, M.; Zhang, Y.; Wang, Y.; Huang, B.; He, Q. Strength, microstructure, efflorescence behavior and environmental impacts of waste glass geopolymers cured at ambient temperature. J. Clean. Prod. 2019, 252, 119610.
52. Tho-In, T.; Sata, V.; Boonserm, K.; Chindaprasirt, P. Compressive strength and microstructure analysis of geopolymer paste using waste glass powder and fly ash. J. Clean. Prod. 2018, 172, 2892–2898.
53. Jiang, X.; Xiao, R.; Ma, Y.; Zhang, M.; Bai, Y.; Huang, B. Influence of waste glass powder on the physico-mechanical properties and microstructures of fly ash-based geopolymer paste after exposure to high temperatures. Constr. Build. Mater. 2020, 262, 120579.